Direct manipulation of atomic excitation with intense extreme-ultraviolet laser fields

Yu He,[1,2,3] Haohan Shi,[1,2] Nan Xue,[1,2] Alexander Magunia,[3] Shaohua Sun,[1,2] Jingjie Ding,[1,2] Bitao Hu,[1,2] and Zuoye Liu[1,2,*]

[1]*Frontiers Science Center for Rare Isotopes, Lanzhou University, 730000 Lanzhou, China*
[2]*School of Nuclear Science and Technology, Lanzhou University, 730000 Lanzhou, China*
[3]*Max-Planck-Institut für Kernphysik, Saupfercheckweg 1, 69117 Heidelberg, Germany*

(Received 26 January 2022; accepted 4 April 2022; published 20 April 2022)

The coherent excitation and manipulation of a two-level system with ultrashort intense extreme-ultraviolet laser fields is investigated theoretically, based on numerically solving the time-dependent Schrödinger equation. We are particularly interested in the dynamical phase excursion of the energy states over the course of the interaction and the resulting spectral modifications. Fitting the absorption line shapes with the Fano profile quantifies the asymmetry parameter and the corresponding dipole phase offset, capturing the phase difference of the state coefficients after the interaction. Nonperturbative analytical calculations using rectangular driving pulses are employed, yielding physical insights into the dependence of the dipole phase shift on the external field. The validity of the formulas is validated by comparing their predictions with numerical results, which proves to be robust against the variation of laser parameters. The present investigation of strong-field dressing effects complements recent attosecond transient absorption studies assuming weak excitation, and marks a ubiquitous phenomenon that should be generally considered for the interaction of matter with intense laser fields.

DOI: 10.1103/PhysRevA.105.043113

I. INTRODUCTION

Time-resolved absorption spectroscopy using ultrashort laser pulses has turned out to be a versatile tool for probing and steering electronic dynamics. High-harmonic generation (HHG) sources have enabled table-top measurements in the extreme-ultraviolet (XUV) region with unprecedented time resolution. Among the many experimental explorations, laser-induced spectral change has been a branch of particular interest. By changing the time delay between the excitation and subsequent modification, the first transient absorption experiment using isolated attosecond pulses to probe the autoionization process demonstrated control over the shape of Fano resonances in 2010 [1]. The follow-up experiment resolved the subcycle ac Stark shift and broadening of the absorption lines of singly excited states of helium [2], proving that bound electrons are able to respond near instantaneously to a perturbing laser field. Ott *et al.* introduced a universal temporal-phase formalism, and revealed the transformation of natural Fano absorption lines into Lorentzian ones and the inverse by adjusting the intensity of the coupling laser [3]. Furthermore, through arranging the transient-absorption scheme in a nonconcentric geometry, the spatial redirection of the XUV pulse has been reported [4,5].

Along with experimental progress, a range of theoretical investigations arise. In addition to directly performing the large-scale *ab initio* description of transient absorption [6–8], endeavors have also been made to devise simplified models which are capable of reproducing the essential spectroscopic characters and seizing the underlying mechanism [2,9–15]. When the coupling laser is not too strong to ionize the medium, the spectral modification is generally conceptualized as the result of a phase excursion $\Delta\phi_j = \int dt\, \Delta E_j$ (atomic units are used unless otherwise noted) on the involved states. These additional phases originating from the corresponding transient energy shift ΔE_j of state j change how the dipole moment oscillates, thereby altering the way the generated radiation adds to the incoming field that promotes the transition. Modifications of resonant profiles in the absorption spectrum occur, which in turn contain information of the dipole oscillation of the system across time. Modeling the energy displacement is thus the central task in this picture, and several approaches have been employed depending on the situations of concern. Ponderomotive energy is justified for loosely bound states [3] and the imprinted information has been utilized in turn to characterize the duration and intensity of laser pulses *in situ* [16]. The ac Stark shift using second-order perturbation theory works well when the coupling field is far off resonant [2,10]. For a near-resonant coupling pulse, computing the energy difference between the dressed bright state and the bare state with the rotating-wave approximation (RWA) in the adiabatic Floquet picture is more appropriate [12].

*zyl@lzu.edu.cn

Most attosecond transient absorption experiments to date employ XUV pulses from table-top HHG sources, whose intensity is relatively low for enabling perturbative treatments. However, modifying the resonant spectral features directly with a single intense driving pulse is possible in the near-infrared (NIR) regime [17,18]. Pioneering works have also proposed the manipulation of autoionization states with intense short-wavelength fields [19–21], which has been demonstrated recently with the employment of state-of-the-art free-electron lasers (FELs) [22]. However, the underlying mechanism for the distortion of the absorption line shapes [22,23] is not unique to multielectron resonances but general for any transitions. The present work focuses on the fundamental resonant interaction of broadband laser pulses with a two-level system, which embodies a simplification of many physical processes. Modulations of the natural absorption line shape are evaluated with respect to a series of pulse parameters, which are further elucidated by an analytical analysis. It is noteworthy to mention that the employed laser field is sufficiently intense to transfer a substantial fraction of population between the states, which necessitates a treatment beyond the perturbation theory. The ponderomotive shift and the adiabatic RWA model mentioned above also fail to capture the strong-field dressing effects as clarified below. The direct manipulation of atomic excitation with intense XUV laser fields is complementary to recent attosecond transient absorption studies treating XUV excitation perturbatively, marking a different way to control electronic dynamics at short wavelengths.

II. METHOD

Our primary interest is to determine the disturbance of atomic energy levels by an intense driving field, and the resulting absorption line-shape changes. Thereby, the description of the quantum system in terms of a wave function is more favorable compared with the density-matrix formalism. We first outline the numerical method for treating the dynamical evolution of a two-level system subjected to an intense laser field. By expanding the wave packet in terms of the field-free states $|\Psi(t)\rangle = c_1(t)e^{-i\omega_1 t}|1\rangle + c_2(t)e^{-i\omega_2 t-\Gamma t/2}|2\rangle$, the variation of the system to the external field is directly encoded in the state coefficients $c_1(t)$ and $c_2(t)$, which could be computed by solving the time-dependent Schrödinger equation formulated as

$$i\dot{c_1}(t) = -\mu E(t)e^{-i\omega_r t-\frac{\Gamma}{2}t}c_2(t), \tag{1a}$$

$$i\dot{c_2}(t) = -\mu E(t)e^{i\omega_r t+\frac{\Gamma}{2}t}c_1(t). \tag{1b}$$

Here, μ denotes the dipole matrix element and $\omega_r = \omega_2 - \omega_1$ is the transition frequency. The electric field is expressed as $E(t) = F(t)e^{i\omega_0 t} + \text{c.c.}$, where $F(t)$ represents the envelope and ω_0 the central frequency. The RWA can be further applied to simplify these differential equations, but we opt for a numerical procedure without it so as to be more accurate, which serves as the baseline for the latter analysis. The single-atom dipole moment can be written as

$$d(t) = \mu c_1(t)c_2^*(t)e^{i\omega_r t-\Gamma t/2} + \text{c.c.} \tag{2}$$

A complete theoretical description of the optical absorbance requires solving the Maxwell wave equation to account for pulse reshaping during propagation through the medium. However, when the target sample is only moderately dense, a full consideration yields similar results with the single-atom calculation, only scaled by the target density [24]. The suppression of propagation effects is beneficial for directly extracting the microscopic response from the absorption spectrum, which is solid to be computed by [6]

$$A(\omega) \propto -\omega\,\text{Im}[\tilde{d}(\omega)/\tilde{E}(\omega)], \tag{3}$$

with $\tilde{d}(\omega)$ and $\tilde{E}(\omega)$ denoting the Fourier transform of the dipole response and the electric field for positive frequencies, respectively. Our Fourier transform convention is $\tilde{d}(\omega) = (1/\sqrt{2\pi})\int_{-\infty}^{\infty} d(t)e^{-i\omega t}dt$.

The asymmetry of the resonant line shape within the absorption $A(\omega)$ is quantified by fitting the Fano profile

$$A(\epsilon) = a\frac{(q+\epsilon)^2}{1+\epsilon^2} + b \tag{4}$$

with the Fano asymmetry parameter q and the reduced energy $\epsilon(\omega) = 2(\omega-\omega_r)/\Gamma$. a and b are fitting parameters for the amplitude and offset, respectively, which are trivial in our discussions. The dipole phase offset is related to the asymmetry parameter by $\phi_d = 2\arg(q-i)$ and in turn $q = -\cot(\phi_d/2)$ [3].

In the temporal domain, the dipole moment consists of two parts: the response during the driving pulse and the ensuing free decay of coherence after the pulse ends. Provided that the decay time of the resonance is much longer than the pulse duration, the main contribution comes from the second process, and the dynamic phase shift accumulated during the interaction can be regarded as an imposed global phase offset. In the limit of perturbative excitation, the dipole emission is π phase shifted with respect to the excitation pulse. The two fields interfere destructively and result in a spectral hole at resonant energy, which manifests as a symmetric Lorentzian profile in the absorption spectrum. When the electronic wave packet is altered during the interaction, a Fano-like dispersive line shape arises, and the field-induced phase changes of the state coefficients can be quantified through the asymmetry change of the absorption profile.

A. General solution for resonant case

When the carrier frequency of the excitation pulse exactly matches the transition frequency, the coupled differential equations (1) can be simplified with the aid of RWA. After disregarding the counter-rotating terms and the decay term as the duration of the laser pulse is much shorter than the decay time of the excited state, we arrive at the following concise forms:

$$i\dot{c_1}(t) = -\tfrac{1}{2}\Omega(t)c_2(t), \tag{5a}$$

$$i\dot{c_2}(t) = -\tfrac{1}{2}\Omega(t)c_1(t). \tag{5b}$$

The Rabi frequency $\Omega(t) = 2\mu F(t)$ appearing here is taken to be real valued. With initial conditions of $c_1(0) = 1$ and

$c_2(0) = 0$, analytical solutions of Eqs. (5) for $t \geqslant 0$ are quite straightforward,

$$c_1(t) = \cos\left[\frac{\theta(t)}{2}\right], \tag{6a}$$

$$c_2(t) = i\sin\left[\frac{\theta(t)}{2}\right], \tag{6b}$$

where $\theta(t) = \int_{-\infty}^{t} \Omega(t')dt'$ denotes the dimensionless time-dependent XUV pulse area. These equations directly show that the evolution of the state coefficients turns out to be independent on the details of the pulse shape, but rather depends solely on its integral. In addition, c_1 is real valued while c_2 is imaginary. Their phase jumps by π when the trigonometric function changes its sign but otherwise remains constant.

B. Solution for near-resonant case driven by a rectangular pulse

When nonzero detuning $\Delta = \omega_0 - \omega_r$ occurs, there is no general analytical solution for the coupled equations. Approximate analytical solutions are only available for certain specific cases. Nevertheless, they contain physical insights into the evolution of the wave packets. A textbook example is the interaction with a near-resonant monochromatic pulse [25]. Based on the formulas, we will show below that the analytical predictions driven by a rectangular pulse, whose amplitude is constant within its duration, prove to be surprisingly accurate for reproducing the numerical calculations computed with a Gaussian driving pulse. Given the initial condition that all population stays in the ground state, the time-dependent coefficients for $T \geqslant t \geqslant 0$ when exposed to a rectangular pulse of duration T with a step turn-on at $t = 0$ are obtained as

$$c_1(t) = e^{i\Delta t/2}\left(\cos\frac{\tilde{\Omega}t}{2} - \frac{i\Delta}{\tilde{\Omega}}\sin\frac{\tilde{\Omega}t}{2}\right), \tag{7a}$$

$$c_2(t) = i\frac{\Omega}{\tilde{\Omega}}e^{-i\Delta t/2}\sin\frac{\tilde{\Omega}t}{2}. \tag{7b}$$

The population of the states oscillates at a frequency $\tilde{\Omega} = \sqrt{\Omega^2 + \Delta^2}$ termed as the generalized Rabi frequency. In terms of dressed energies, these expressions can be further written as

$$c_1(t) = \frac{\tilde{\Omega} - \Delta}{2\tilde{\Omega}}e^{i(\tilde{\Omega}+\Delta)t/2} + \frac{\tilde{\Omega} + \Delta}{2\tilde{\Omega}}e^{-i(\tilde{\Omega}-\Delta)t/2}, \tag{8a}$$

$$c_2(t) = \frac{\Omega}{2\tilde{\Omega}}e^{i(\tilde{\Omega}-\Delta)t/2} - \frac{\Omega}{2\tilde{\Omega}}e^{-i(\tilde{\Omega}+\Delta)t/2}. \tag{8b}$$

We note that these equations for the resonant case of $\Delta = 0$ are equivalent to Eqs. (6) when the Rabi frequency is constant. From the structure of the above expressions, two sideband frequencies are present around each field-free energy when the driving pulse turns on. The ground state contains frequencies $(-\Delta \pm \tilde{\Omega})/2$, and the excited state $(\omega_0 \pm \tilde{\Omega})/2$ with equal strength. If the transition is probed by a weak laser from a third level across any of the two states, then the splitting of the energy levels can be measured, which is commonly referred to as the Autler-Townes effect [26]. When the system is subject to steady illumination, a Mollow triplet appears in the fluorescence spectrum [27]. The phase difference between the state coefficients when the pulse ends is expressed as

$$\begin{aligned}\Delta\varphi &= \arg[c_2(T)c_1^*(T)] \\ &= \arg\left\{e^{-i\Delta T}\left[i\sin\tilde{\Omega}T - \frac{\Delta}{\tilde{\Omega}}(1-\cos\tilde{\Omega}T)\right]\right\}.\end{aligned} \tag{9}$$

Subtracting its counterpart in the weak-field limit ($\tilde{\Omega} \to \Delta$) directly yields the phase shift induced by the interaction, which translates into the change of absorption line shapes.

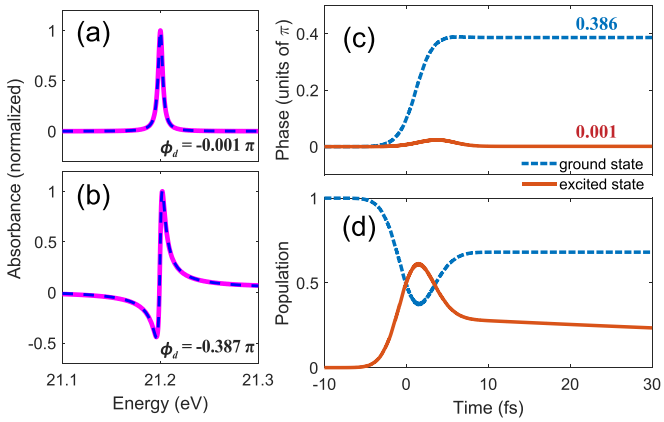

FIG. 1. Normalized absorption line shapes calculated numerically (magenta solid lines) with a Gaussian pulse centered at 21.0 eV ($\Delta = -0.2$ eV) for peak intensities of (a) 0.1×10^{12} W/cm^2 and (b) 35×10^{12} W/cm^2. Fitting of them (blue dashed lines) reveals the asymmetry parameter and corresponding dipole phase shift. Time evolution of the (c) phase shifts and (d) populations of the ground and excited states with the same laser parameters as in (b). The labeled values denote the phase shifts after the interaction.

III. RESULTS AND DISCUSSIONS

A. Analysis of the spectral modification

Our simulations are exemplified by the isolated excitation and transient modification of the $1s^2$ to $1s2p$ transition of helium, whose spectral signature has been extensively investigated in recent attosecond transient absorption studies [10–13,15,24,28,29]. Furthermore, as the lowest excitation state of helium, the $2p$ electron is far from being regarded as free to employ the ponderomotive energy shift. The ground-state energy ω_1 is taken as zero, and the field-free energy of the excited state ω_2 is 21.2 eV. The dipole matrix element μ is 0.4, and a decay time $1/\Gamma$ of 120 fs is assumed. For the numerical results shown below, we use Gaussian driving pulses of $\tau = 5$ fs full width at half maximum (FWHM) duration for demonstration unless otherwise specified. In our calculations, the pulse area θ of 0–1.5π is chosen to induce notable Rabi oscillations between the states, while the laser field (maximum peak intensity of 50×10^{12} W/cm^2) is not too strong to ionize the upper state so that the two-level consideration retains.

Figures 1(a) and 1(b) show the absorption profiles driven by a single XUV pulse with a carrier frequency of 21.0 eV for two typical pulse intensities. The absorption line shape remains Lorentzian when the pulse is relatively weak in Fig. 1(a), and the fitting quantifies a negligible dipole phase

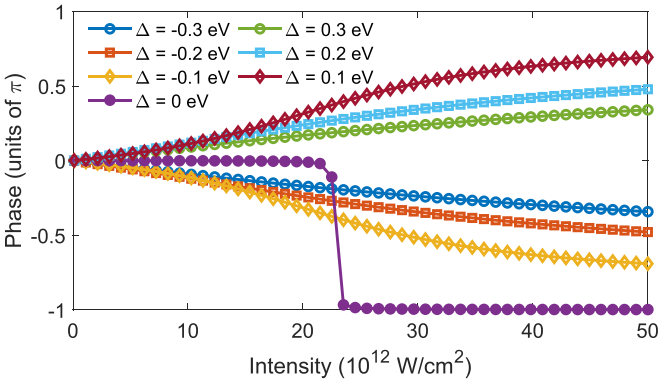

FIG. 2. Dipole phase shifts retrieved from fitting the numerical absorption line shapes as a function of laser intensity for different detunings.

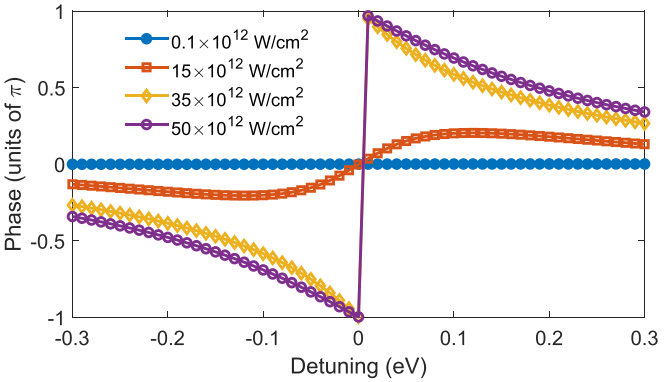

FIG. 3. Retrieved dipole phase shifts as a function of detuning for fixed laser intensities.

shift. By contrast, the stronger pulse induces a remarkable spectral modification, and an asymmetric Fano-like profile is exhibited in Fig. 1(b). For the latter case, we plot the phase evolution of the state coefficients $\phi_i(t) = \arg[c_i(t)]$ in Fig. 1(c), which may be further related to the transient energy shift of the states during the interaction. The trivial phase evolution when driven by a very weak field has been subtracted, and the results directly represent the phase excursion induced by the external field. The extracted dipole phase shift ϕ_d through fitting the line shape agrees well with the calculated value $\phi_2 - \phi_1$ after interaction with the pulse, confirming that the modification of the absorption line shape indeed originates from the field dressing of the states. The initial accumulation of the phase shifts arising from the finite pulse duration prevents us from achieving better agreement, which depends on the details of excitation and is not captured with the single asymmetry parameter q of the line shape (or equivalent global phase offset ϕ_d). The significant modification of the absorption line shape is accompanied by a remarkable population transfer between the states, which is presented in Fig. 1(d). This observation clearly evidences the necessity of going beyond the weak-excitation scenario, and approaches based on the perturbation theory are inherently inapplicable.

After connecting the spectral line-shape change to the phase shifts of the states, we proceed to explore these phenomena in more general cases by varying the key parameters of the driving XUV field. Figure 2 shows the extracted dipole phase offset ϕ_d as a function of pulse intensity with detunings ranging from -0.3 to 0.3 eV. For resonant driving pulse, the phase shift remains zero before experiencing an abrupt jump to $-\pi$ at a critical intensity, corresponding to a spectral line shape change from Lorentzian to inverted Lorentzian; this novel phase jump stays concealed with the insufficient pulse intensity employed in Ref. [23]; the $-\pi$ phase persists as the intensity further grows. By contrast, these values for near-resonant cases evolve monotonically with increasing laser intensity. The phase shifts for negative and positive detuning with an identical amount share approximately the same amplitude but with opposite signs (positive phase shift for blue detuning and negative for red detuning), and larger detuning from the resonance generally induces a smaller degree of shifts.

Figure 3 presents how the extracted dipole phase shift evolves with varying detuning for four representative pulse intensities. As expected, the weak laser pulse barely modifies the state coefficients and hence the absorption line shape, appearing as a zero phase shift across the detuning range. For a higher pulse intensity, the phase evolves smoothly and crosses zero at the resonant position, while the induced modification is still moderate. When the driving pulse is even more intense, inverse-proportional-function-like curves are exhibited. The phase declines gradually to $-\pi$ as detuning increases from negative to zero, and a steady decrease from π follows with increasing positive detuning.

These observations can be understood with the aid of the analytical formulas given above. Each state transforms into two dressed states when the driving pulse is on. In XUV-NIR transient-absorption scenario, the NIR pulse strongly couples a two-level system, which is probed by the XUV pulse; the stronger part in Eq. 8(a) accounts for the Stark-shifted bright state, while the weak part explains the appearance of a light-induced state. By virtue of the adiabatic RWA model, the phase gain calculated from the energy difference between the dressed state and the bare state works well for capturing the line-shape changes of the bright state in transient-absorption spectra [12]. Nevertheless, directly employing it in the present case is impractical as the transient splitting occurs on a timescale considerably shorter than the ensuing free decay, and no spectral shift and splitting manifest in the absorption spectrum as a result of the Fourier transform. It has also been pointed out before, implicitly or explicitly, that the estimation of the light-induced energy shift via the generalized Rabi frequency breaks down when driven by ultrashort laser fields [22,23]. This becomes clear as each term on the right-hand side of Eqs. (8) is unable to fully account for the phase change of the corresponding state coefficients, and the dipole phase shift resulting from the whole contribution should be evaluated through Eq. (9). The phase evolution for the on-resonance condition becomes much more intuitive with the help of Eqs. (6) general for any pulse shape. The ground-state coefficient changes its phase by π (i.e., its amplitude changes sign) when the pulse area crosses π with increasing pulse intensity, and remains constant for other cases. By contrast, the phase of the excited state coefficient stays unchanged for the employed pulse area range of 0–1.5π. Equations (6) also

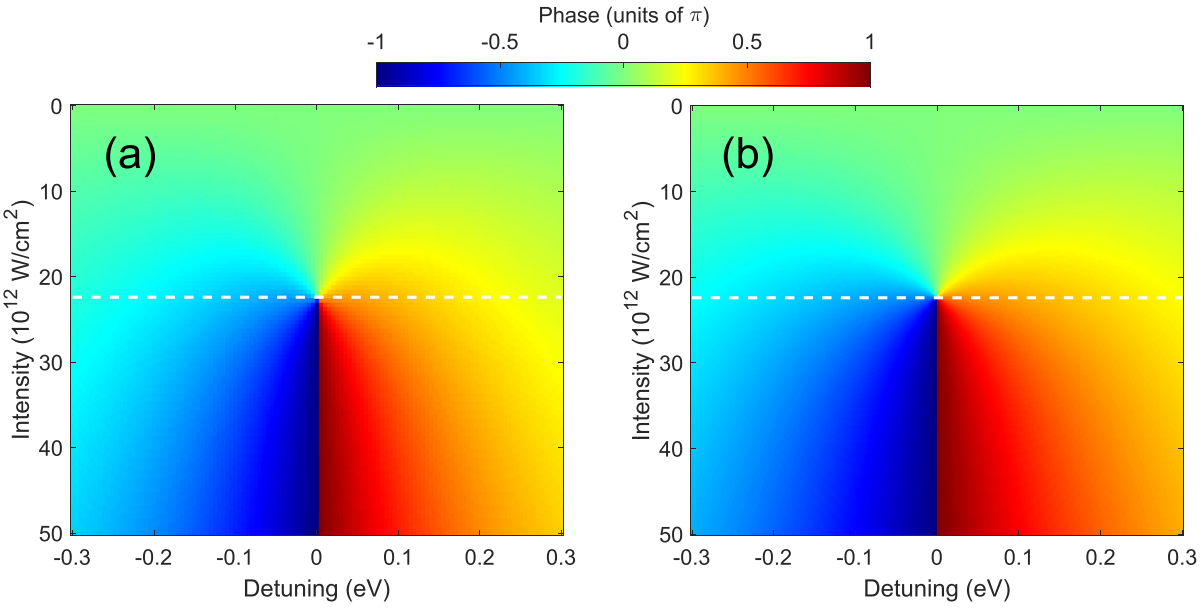

FIG. 4. Dipole phase shifts (a) retrieved from numerical spectra using a Gaussian driving pulse and (b) calculated analytically with a rectangular pulse. In the calculation, the pulse area of the rectangular pulse is chosen to be identical to that of the Gaussian pulse. To enable comparison, the intensity at which the pulse area equals π is indicated with dashed lines.

imply that the phase change of the coefficient from 0 to π occurs instantaneously in the time domain, which has been validated by numerical calculation with RWA (not shown). This observation indicates that the returning electrons to the ground state after completing half a Rabi cycle carry an additional phase of π, and the picture of the transient energy shift breaks down. The result without RWA assumes a short rise time, proving the deviation stems from the dropped counter-rotating terms in the original differential equations (1). The dipole phase shifts resulting from the analytical model for the detuning range are shown in Fig. 4 together with the values retrieved from the numerical absorption spectra. In our analytical calculation, the amplitude of the electric field is chosen to match the peak electric field of the Gaussian pulse in the numerical calculation while keeping an identical pulse area, yielding a rectangular pulse duration $T = \tau\sqrt{\pi/(2\ln 2)}$. A heartlike (or fountainlike) overall profile is exhibited, which is symmetric around the resonant position. The analytical predictions accord closely with the extracted results, serving as a quantitative guide to how the laser-induced phase and the resulting absorption profile evolve with varying driving pulse intensity and central frequency.

B. Effect of laser duration

As mentioned, all results discussed so far have been calculated with a relatively short pulse duration. In addition to the intensity and central frequency, the pulse duration is another important factor of the driving pulse that merits careful consideration. Below we intend to show the robustness of the analytical model against the variation of the driving pulse duration. In Fig. 5(a), we compare the dipole phase shifts obtained by numerical and analytical calculations, and by fitting the numerical absorption line shapes as a function of input Gaussian pulse duration. Considering the narrow spectral bandwidth for even longer laser pulses, the pulse duration is chosen up to 10 fs. For a fixed peak pulse intensity, a longer pulse duration corresponds to a larger pulse area. The

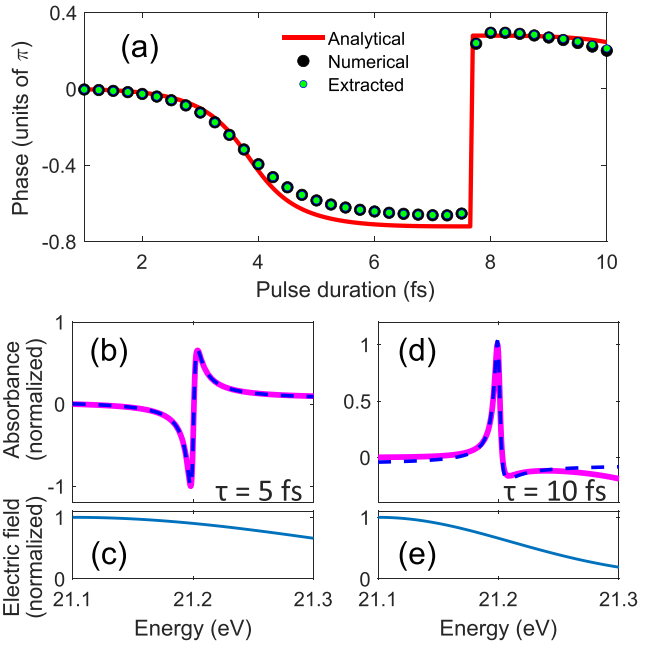

FIG. 5. (a) The dipole phase shifts calculated analytically and numerically, and extracted from the numerical absorption spectra with varying pulse duration. The pulse intensity and central photon energy of the driving laser are fixed at 35×10^{12} W/cm^2 and 21.1 eV, respectively. (b), (d) Numerical absorption line shapes (magenta solid lines) and fitting of them (blue dashed lines) for the case of 5 and 10 fs pulse duration. The corresponding electric fields (magnitude) in the frequency domain are shown in (c) and (e).

magnitude of the dipole phase shift rises initially as the pulse duration increases, showing a similar trend with increasing intensity as shown in Fig. 2. Further increases of the duration witness an abrupt phase change of π. Taking a closer look at Eq. 7(a), one can easily conclude that the excited state coefficient changes its phase sharply by π when the generalized pulse area $\tilde{\Omega}t$ exceeds the critical value of 2π, corresponding to a rectangular pulse duration $T = 11.55$ fs for the employed laser parameters and a Gaussian pulse duration τ of 7.67 fs, in excellent accord with our observation. The general agreement with the numerical calculations over the pulse duration range validates again the efficiency of the analytical model, addressing the influence of strong laser fields to the energy states and the pulse aftermath in the absorption spectrum. It is worth mentioning that when the driving pulse is rather long, its electric field in the frequency domain differs considerably in the vicinity of the resonance owing to the narrow bandwidth. The spectral characteristic resulting from Eq. (3) deviates from the well-defined Fano-like profile, especially in the wings, making the extracted phase shift less accurate.

C. Effect of chirp

Until now only the dynamics driven by Fourier transform-limited laser pulses has been considered. However, the chirp characteristic of the laser pulse, either intrinsic due to the nonlinear generation process or acquired in the course of passing through the optical path, is difficult to eliminate and will affect the light-matter interaction [30–32]. Finally, we briefly consider the simplest case of a linearly chirped driving pulse, i.e.,

$$E(t) = F(t)e^{i\omega_0 t + ict^2/2} + \text{c.c.} \tag{10}$$

The instantaneous frequency of the laser pulse is related to the chirp rate c by $\omega = \omega_0 + ct$. We restrict our discussion to laser pulses with a central frequency ω_0 exactly match the transition frequency ω_r, such that the red- and blue-detuned parts are symmetrically located around the pulse center with equal strength. Figure 6 presents the dipole phase shifts extracted from numerical absorption line shapes for a fixed pulse duration of 5 fs and a set of chirp parameters. Recalling our above conclusion that the red- and blue-detuned pulses with an equal detuning amount induce the same amplitude of the dipole phase shift but with reverse signs, and taking the chirped laser pulse as a series of "chirp-free" subpulses in time with varying carrier frequency, a phenomenological understanding of the process is present. When the driving pulse is weak that the depopulation of the ground state is slight, the phase excursion induced by the red-detuned part counteracts that of the blue-detuned part, making no net phase shift left after the interaction. The increase of the amplitude of the dipole phase with intensity implies the deviation from the approximation. The chirp-free subpulses interact with the atoms sequentially in the time domain and face different initial conditions, making the involved dynamics more complicated than the simple analysis. Nevertheless, the induced dipole modifications in most cases are largely suppressed compared with the chirp-free excitation case as shown before in Fig. 2. Further rises of the pulse intensity witness a sharp dipole phase step of around π for small chirp rates, which may be linked to the higher contribution of small-detuned frequency parts contained in the driving pulse. Such a manipulation scenario should be experimentally feasible, as chirped XUV pulses are routinely produced through the high-harmonic generation [33], or the FEL generation process when aiming at a broad photon bandwidth [32].

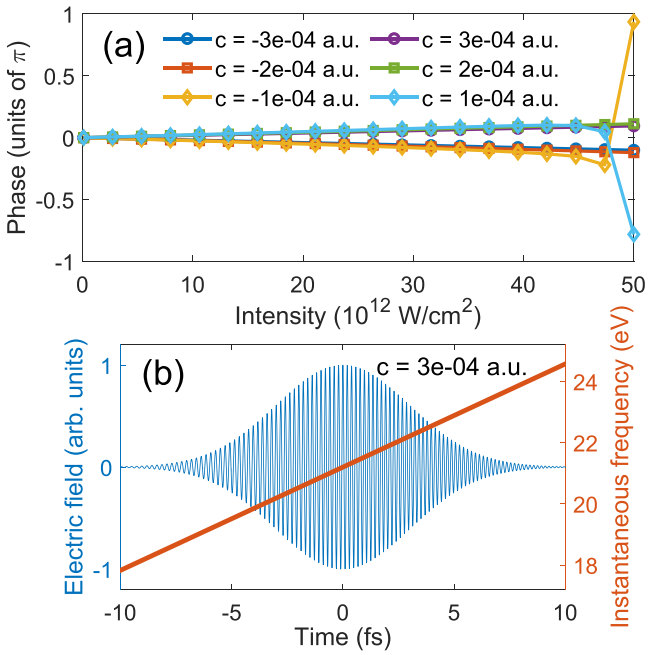

FIG. 6. (a) The extracted dipole phase as a function of pulse intensity for a set of chirp parameters. (b) Example of the evolution of a chirped electric field and its instantaneous frequency with time.

IV. CONCLUSIONS

In summary, the direct manipulation of bound-state dynamics with intense XUV fields has been demonstrated. The asymmetry change of the absorption profile encodes field-induced phase shifts of the dipole oscillation and the associated states. The dipole phase offset reveals an abrupt change when the (generalized) pulse area meets certain conditions. Our results validate that the analytical model captures much of the line-shape dynamics, in terms of the phase excursion of the involved state coefficients, allowing one to make a quick estimation of the laser modification from given pulse parameters by using Eq. (9). To facilitate the extraction of dynamics and enable better agreement with the analytical model, the utilization of broadband driving pulses with a temporal duration much shorter than the lifetime of the resonance is favorable. The presented scheme is generally relevant for accessing and controlling electronic dynamics at short wavelengths, which circumvents the need for another pulse, as commonly done in transient absorption studies. Further manipulation of the dynamics could be afforded by changing the atomic density, which goes beyond the single-atom approximation. The extension of the present work to involve more energy levels is potentially valuable for more realistic cases, albeit with a scaling in complexity.

ACKNOWLEDGMENTS

This work was supported by the National Natural Science Foundation of China (Grants No. U1932133, No. 11905089, and No. 12027809), the Natural Science Foundation of Gansu Province (Grant No. 20JR5RA222), the funding for excellent postgraduates granted by the Department of Education of Gansu Province (Grant No. 2021CXZX-015), and Supercomputing Center of Lanzhou University. Y.H. acknowledges the support from the China Scholarship Council.

[1] H. Wang, M. Chini, S. Chen, C.-H. Zhang, F. He, Y. Cheng, Y. Wu, U. Thumm, and Z. Chang, Attosecond Time-Resolved Autoionization of Argon, Phys. Rev. Lett. **105**, 143002 (2010).

[2] M. Chini, B. Zhao, H. Wang, Y. Cheng, S. X. Hu, and Z. Chang, Subcycle ac Stark Shift of Helium Excited States Probed with Isolated Attosecond Pulses, Phys. Rev. Lett. **109**, 073601 (2012).

[3] C. Ott, A. Kaldun, P. Raith, K. Meyer, M. Laux, J. Evers, C. H. Keitel, C. H. Greene, and T. Pfeifer, Lorentz meets Fano in spectral line shapes: A universal phase and its laser control, Science **340**, 716 (2013).

[4] S. Bengtsson, E. W. Larsen, D. Kroon, S. Camp, M. Miranda, C. L. Arnold, A. L'Huillier, K. J. Schafer, M. B. Gaarde, L. Rippe, and J. Mauritsson, Space–time control of free induction decay in the extreme ultraviolet, Nat. Photonics **11**, 252 (2017).

[5] E. R. Simpson, M. Labeye, S. Camp, N. Ibrakovic, S. Bengtsson, A. Olofsson, K. J. Schafer, M. B. Gaarde, and J. Mauritsson, Probing Stark-induced nonlinear phase variation with opto-optical modulation, Phys. Rev. A **100**, 023403 (2019).

[6] M. B. Gaarde, C. Buth, J. L. Tate, and K. J. Schafer, Transient absorption and reshaping of ultrafast XUV light by laser-dressed helium, Phys. Rev. A **83**, 013419 (2011).

[7] C. Ott, A. Kaldun, L. Argenti, P. Raith, K. Meyer, M. Laux, Y. Zhang, A. Blättermann, S. Hagstotz, T. Ding *et al.*, Reconstruction and control of a time-dependent two-electron wave packet, Nature (London) **516**, 374 (2014).

[8] L. Argenti, A. Jiménez-Galán, C. Marante, C. Ott, T. Pfeifer, and F. Martín, Dressing effects in the attosecond transient absorption spectra of doubly excited states in helium, Phys. Rev. A **91**, 061403(R) (2015).

[9] A. N. Pfeiffer and S. R. Leone, Transmission of an isolated attosecond pulse in a strong-field dressed atom, Phys. Rev. A **85**, 053422 (2012).

[10] S. Chen, M. Wu, M. B. Gaarde, and K. J. Schafer, Laser-imposed phase in resonant absorption of an isolated attosecond pulse, Phys. Rev. A **88**, 033409 (2013).

[11] M. Wu, S. Chen, M. B. Gaarde, and K. J. Schafer, Time-domain perspective on Autler-Townes splitting in attosecond transient absorption of laser-dressed helium atoms, Phys. Rev. A **88**, 043416 (2013).

[12] M. Wu, S. Chen, S. Camp, K. J. Schafer, and M. B. Gaarde, Theory of strong-field attosecond transient absorption, J. Phys. B: At., Mol. Opt. Phys. **49**, 062003 (2016).

[13] J. J. Rørstad, J. E. Bækhøj, and L. B. Madsen, Analytic modeling of structures in attosecond transient-absorption spectra, Phys. Rev. A **96**, 013430 (2017).

[14] K. Mi, W. Cao, H. Xu, Y. Mo, Z. Yang, P. Lan, Q. Zhang, and P. Lu, Perturbed ac Stark Effect for Attosecond Optical-Waveform Sampling, Phys. Rev. Appl. **13**, 014032 (2020).

[15] X. Wu, Z. Yang, S. Zhang, X. Ma, J. Liu, and D. Ye, Buildup time of Autler-Townes splitting in attosecond transient absorption spectroscopy, Phys. Rev. A **103**, L061102 (2021).

[16] A. Blättermann, C. Ott, A. Kaldun, T. Ding, V. Stooß, M. Laux, M. Rebholz, and T. Pfeifer, In situ characterization of few-cycle laser pulses in transient absorption spectroscopy, Opt. Lett. **40**, 3464 (2015).

[17] J. K. Ranka, R. W. Schirmer, and A. L. Gaeta, Coherent spectroscopic effects in the propagation of ultrashort pulses through a two-level system, Phys. Rev. A **57**, R36 (1998).

[18] Y. He, Z. Liu, Z. Cui, Y. Zhang, A. N. Pfeiffer, T. Pfeifer, J. Ding, and B. Hu, Signatures of self-modulation effects during pulse propagation in single-pulse absorption spectra, Phys. Rev. A **99**, 053418 (2019).

[19] P. Lambropoulos and P. Zoller, Autoionizing states in strong laser fields, Phys. Rev. A **24**, 379 (1981).

[20] A. N. Artemyev, L. S. Cederbaum, and P. V. Demekhin, Impact of intense laser pulses on the autoionization dynamics of the $2s2p$ doubly excited state of He, Phys. Rev. A **96**, 033410 (2017).

[21] G. Mouloudakis and P. Lambropoulos, Autoionizing states driven by stochastic electromagnetic fields, J. Phys. B: At., Mol. Opt. Phys. **51**, 01LT01 (2017).

[22] C. Ott, L. Aufleger, T. Ding, M. Rebholz, A. Magunia, M. Hartmann, V. Stooß, D. Wachs, P. Birk, G. D. Borisova, K. Meyer, P. Rupprecht, C. da Costa Castanheira, R. Moshammer, A. R. Attar, T. Gaumnitz, Z.-H. Loh, S. Düsterer, R. Treusch, J. Ullrich, Y. Jiang, M. Meyer, P. Lambropoulos, and T. Pfeifer, Strong-Field Extreme-Ultraviolet Dressing of Atomic Double Excitation, Phys. Rev. Lett. **123**, 163201 (2019).

[23] A. Magunia, L. Aufleger, T. Ding, P. Rupprecht, M. Rebholz, C. Ott, and T. Pfeifer, Bound-state electron dynamics driven by near-resonantly detuned intense and ultrashort pulsed XUV fields, Appl. Sci. **10**, 6153 (2020).

[24] S. Chen, M. J. Bell, A. R. Beck, H. Mashiko, M. Wu, A. N. Pfeiffer, M. B. Gaarde, D. M. Neumark, S. R. Leone, and K. J. Schafer, Light-induced states in attosecond transient absorption spectra of laser-dressed helium, Phys. Rev. A **86**, 063408 (2012).

[25] R. W. Boyd, *Nonlinear Optics* (Academic, New York, 2020).

[26] S. H. Autler and C. H. Townes, Stark effect in rapidly varying fields, Phys. Rev. **100**, 703 (1955).

[27] B. R. Mollow, Power spectrum of light scattered by two-level systems, Phys. Rev. **188**, 1969 (1969).

[28] S. Chen, M. Wu, M. B. Gaarde, and K. J. Schafer, Quantum interference in attosecond transient absorption of laser-dressed helium atoms, Phys. Rev. A **87**, 033408 (2013).

[29] M. Wu, S. Chen, K. J. Schafer, and M. B. Gaarde, Ultrafast time-dependent absorption in a macroscopic three-level helium gas, Phys. Rev. A **87**, 013828 (2013).

[30] H. Zhao, C. Liu, Y. Zheng, Z. Zeng, and R. Li, Attosecond chirp effect on the transient absorption spectrum of laser-dressed helium atom, Opt. Express **25**, 7707 (2017).

[31] J. Xue, C. Liu, Y. Zheng, Z. Zeng, R. Li, and Z. Xu, Infrared-laser-induced ultrafast modulation on the spectrum of an extreme-ultraviolet attosecond pulse, Opt. Express **26**, 9243 (2018).

[32] T. Ding, M. Rebholz, L. Aufleger, M. Hartmann, V. Stooß, A. Magunia, P. Birk, G. D. Borisova, D. Wachs, C. da Costa Castanheira *et al.*, Measuring the frequency chirp of extreme-ultraviolet free-electron laser pulses by transient absorption spectroscopy, Nat. Commun. **12**, 643 (2021).

[33] T. Sekikawa, T. Ohno, T. Yamazaki, Y. Nabekawa, and S. Watanabe, Pulse Compression of a High-Order Harmonic by Compensating the Atomic Dipole Phase, Phys. Rev. Lett. **83**, 2564 (1999).